Modeling the bandwidth of perceptual experience using deep convolutional neural networks

Michael A. Cohen[1,2], Kirsten O. Lydic[1], & N. Apurva Ratan Murty[1]

[1] McGovern Institute for Brain Research, Department of Brain and Cognitive Sciences, Massachusetts Institute of Technology

[2] Department of Psychology and Program in Neuroscience, Amherst College

Abstract

When observers glance upon a natural scene, which aspects of that scene ultimately reach perceptual awareness? To answer this question, we showed observers images of scenes that had been altered in numerous ways in the periphery (e.g., scrambling, rotating, filtering, etc.) and measured how often these different alterations were noticed in an inattentional blindness paradigm. Then, we screened a wide range of deep convolutional neural network architectures and asked which layers and features best predict the rates at which observers noticed these alterations. We found that higher-level layers/features predicted how often observers noticed different alterations with extremely high accuracy (i.e., at the noise ceiling). This suggests that the extent to which observers noticed alterations to a scene depend on the extent to which higher-level features of a scene were preserved or changed. These findings suggest that perceptual awareness is limited by higher-level features of the human visual system.

Introduction

How much information do observers perceive when looking at a natural scene? Is their experience of the world rich and detailed (Lamme, 2003; Block, 2011; Haun et al., 2017), or is it sparse and limited (Dehaene and Changeux, 2011; Cohen et al., 2012; Knotts et al., 2019)? What specific aspects of the visual world are observers aware of at any given moment? To try and answer these questions, researchers often use paradigms like change and inattentional blindness to examine the limits of perceptual experience (Jensen et al., 2011). In typical versions of these experiments, individual items change or appear in some unexpected manner and researchers measure how often observers notice these events. From these results, researchers try to infer the amount of information that ultimately reaches perceptual awareness.

Although these paradigms have yielded numerous important findings, there are limits as to what can be gleaned about the nature of perceptual experience using this approach for two main reasons. The first reason is that the changes that typically occur in these experiments involve alterations that are confined to individual objects/people within complex scenes: a shadow that appears and disappears (Rensink et al., 1997), a rail in the background that moves up and down (O'Regan et al., 1999), an individual in a gorilla costume that walks amongst a group of people (Simons et al., 1999), etc. Although these examples are undoubtedly striking, it is difficult to extrapolate from these findings to broad generalizations about the overall bandwidth of perceptual experience. For instance, what does it mean if an observer fails to notice a shadow appearing and disappearing? Does it mean that their perception of the scene is limited to just a handful of items and no broader information about the scene is perceived (Mack & Rock, 1997; Simons et al., 2005; Cohen et al., 2011)? Or, alternatively, do observers still have a general sense of the gist of world around them and are simply unaware of relatively smaller details within a scene (Cohen et al., 2016; Rosenholtz, 2020)? Or, perhaps observers are aware of the shadow appearing and disappearing, but simply do not have the capacity to report or remember that fact (Wolfe, 1999; Lamme, 2003; Block, 2011; Haun et al., 2017)? The fact that there are so many different interpretations of these data highlights the difficulties in reaching firm conclusions using this standard approach.

The second limitation to the standard approach is because the items that change in these paradigms do so along vastly different dimensions, making it difficult to synthesize them into a coherent whole. For example, the critical manipulations in these experiments involve a wide array of stimuli ranging from lower-level items like colors and simple shapes (Rensink et al., 1997; Luck and Vogel, 1997; Mack & Rock, 1997; Most et al., 2005; Ward et al., 2015; Drew & Stothart, 2016), to complex objects (Fisher et al., 1980; Simons et al., 2000; Levin et al., 2000; Chabris et al., 2011; Jensen et al., 2011) or even entire scenes (Cohen et al., 2011; Mack & Clarke, 2012). Therefore, creating general principles about perceptual experience from this diverse set of studies is difficult since the manipulated variables fall along numerous different perceptual dimensions.

With these two factors in mind, we took a different approach to examining the limits of perceptual awareness. Here, we first altered images of natural scenes in numerous ways: scrambling the periphery so much that no object can be identified, putting the periphery

through a low-pass filter, rotating the periphery 180°, etc. Then, we quantified how often observers noticed these different alterations in an inattentional blindness paradigm using Amazon's Mechanical Turk (N=1,260 observers). Critically, however, we then sought to unify these behavioral results by building computational models based on deep convolutional neural networks (dCNNs) that could predict the behavioral inattentional blindness rates. The idea behind this approach is that by building models that predict observers' behavior, we could then probe the internal features of these computational models to infer the critical features that best predicted performance.

The first question we asked from this modelling approach was, which specific dCNN layers and features best predict behavioral performance? One possibility is that earlier layers and lower-level features are sufficient to predict human inattentional blindness rates. This prediction comes from the fact that many prior studies have found that models of early vision can predict performance on a variety of visual tasks such as crowding (Balas et al., 2009; Freeman and Simoncelli, 2011), visual search (Itti & Koch, 2000; Zhang et al., 2015), scene perception (Oliva & Torralba, 2001; 2006), and even change blindness (Rosenholtz, 2020). Alternatively, higher-level features may best predict behavior, with several prior studies showing a direct relationship between later layers of neural networks and a variety of visual behaviors such as similarity judgements (Kubilius et al., 2016; Jozwik et al., 2013; Cichy et al., 2019), object recognition (Rajalingham et al., 2018), the attentional blink (Lindh et al., 2019), and face perception (Farzmahdi et al., 2016; Jacob et al., 2021). Finally, it is also possible that a combination of both higher- and lower-level features will best predict behavior, with observers using a combination of both higher- or lower-level cues to detect alterations to the periphery depending on the stimuli.

To preview the results, across 7 neural network model architectures, we found that later, but not earlier, dCNN layers could predict how frequently observers noticed different alterations to an image with extremely high accuracy, accounting for all of the explainable behavioral variance. Probing this result further, we found that a very small fraction of model features within the later layers are both necessary and sufficient to predict the human inattentional behavioral rates. Finally, we used visualization methods to directly examine the specific features that primarily drive the predictive power of these models. Overall, these features were highly complex and largely represented the contours of objects (e.g., chairs, couches, people, etc.) and the largest contours of a scene (e.g., the horizon, the shoreline, etc.). Taken together, these results indicate that a small number of higher-level visual features play a crucial role in determining the bandwidth of perception and showcases a powerful alternate computational strategy to infer the computations that constrain the bandwidth of human visual perception.

Results

Inattentional blindness paradigm

All of the methods and analyses procedures were pre-registered and can be found at the following link: osf.io/zr3ed. Overall, we created 21 experimental conditions with each condition corresponding to a different way of altering the periphery (Figure 1; see

Supplemental Figures 1 & 2 for visualization of stimulus creation for more examples; see Methods for more detail on the stimuli).

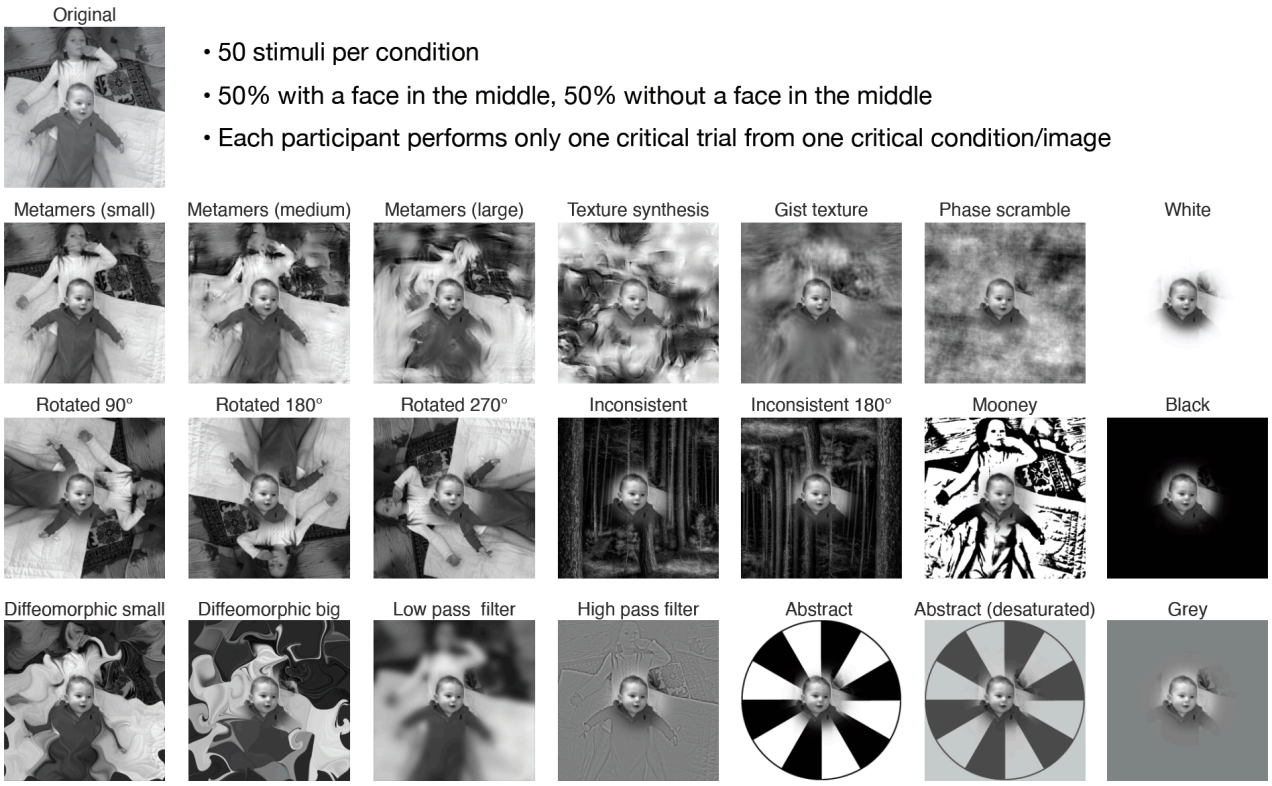

Figure 1. Stimuli. Examples from each experimental condition. An original image is shown on the top left, with an example of that image then being altered in each of the 21 different experimental condition.

The inattentional blindness methods were modelled after those used in Cohen et al. (2020; 2021). Participants were unaware of the experiment's true nature and were instructed to perform a simple face detection task at fixation (see Methods). On each trial, participants were shown 7-30 images of natural scenes and reported whether the last image they saw in the stream contained a face in the middle of it (Figure 2a). Each image was shown for 288ms with a 100ms gap in between. We chose this presentation rate because an analysis of several eye-tracking studies revealed that this is approximately the duration of a single fixation period in naturalistic viewing conditions (Rayner, 1998; Pelz & Canosa, 2001; Hayhoe et al., 2003; Henderson, 2003; Unema et al., 2005; Rayner et al., 2008; Castelhano & Heaven, 2011; Nuthmann, 2017). Regardless of whether or not the trial had a face at the end of it, there were anywhere between 2 and 5 images that had faces in the middle of them throughout the stream. Participants were explicitly told that this would happen and that they were only to say whether or not the *last* image in a given trial had a human face in the middle. No image was ever seen twice within a single trial, although images could be seen multiple times across trials. However, the images that were altered on the inattentional blindness trials were never shown before the critical trial. For the first 10 trials, half of the trials had a face target present at the end and half did not. At the end of each trial, a screen appeared that prompted the observer to say whether or not the last image had a human face in the

middle. Observers pressed one key to report that a target face was present and another key to report that no target face was present.

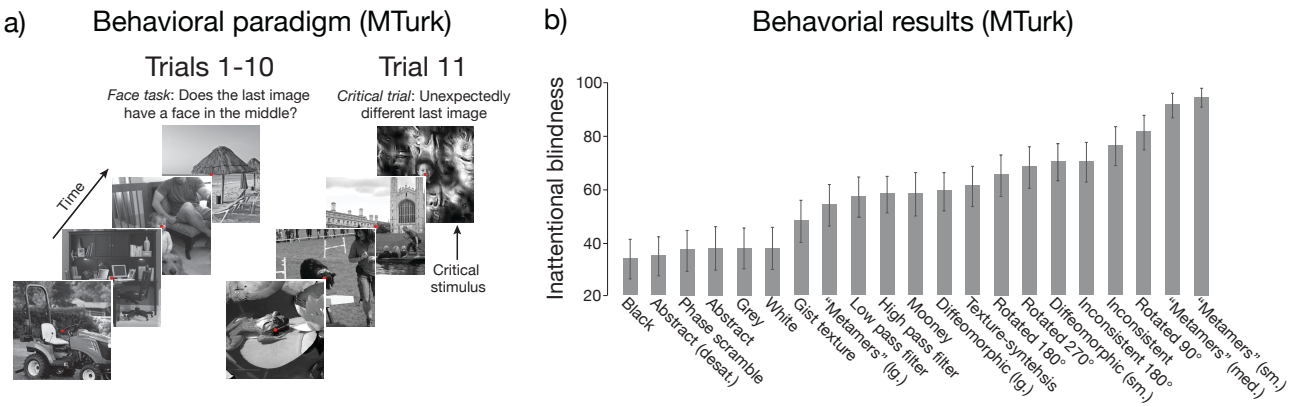

Figure 2. Behavioral experiment and results. a) Visualization of the trial procedures for the behavioral experiment. Participants performed 10 trials where they simply said if the last image in the stream did or did not contain a human face in the middle. Then, on trial 11, an unexpected critical stimulus was presented at the end of the trial and participants were immediately probed to determine whether or not they noticed the critical stimulus. b) Inattentional blindness rates for each condition in the behavioral experiment. The percentage of participants who failed to notice the critical stimulus is plotted on the vertical axis. Each bar corresponds to a different experimental condition. The error bars represent bootstrapped standard errors.

On the critical trial, the very last image in the stream was a critical target stimulus (Figure 1). Within every experimental condition, half of the participants were shown a critical stimulus with a human face in the middle and the other half were shown a critical stimulus that did not have a human face in the middle. As soon as the critical stimulus disappeared, rather than be asked about if a face was in the middle, observers were instead asked another series of questions. Specifically:

1) "Did you notice anything strange or different about that last trial?"
2) "If we were to tell you there was something different about that last trial, could you say what it was?"
3) "If we were to tell you there was something different about the very last image you saw on that last trial, could you say what it was?"

Only those participants who responded "no" to all of these questions were classified as having been inattentionally blind to the alterations. If an observer responded "yes" to any of these questions, they were classified as having noticed the alterations.

The results from these behavioral experiments are plotted in Figure 2b. Overall, there is substantial variance in the inattentional blindness rates between conditions. For example, virtually no observers noticed when the periphery was altered in the small and medium "metamer" conditions (91% and 92.5% rates of inattentional blindness respectively), while many observers noticed when the periphery was black or abstract and desaturated (34% and 35% rates of inattentional blindness respectively). This difference in inattentional blindness rates across conditions is important as it provides us with an opportunity to try and account for this variance using dCNNs. The participants were also highly consistent in their responses (Spearman-Brown corrected, split-half reliability r=0.82, P<0.00001). However, before attempting to model these results, it is also important to first examine the reliability of

the data that we obtained using MTurk compared to our in-lab studies. To answer this question, we directly compared the inattentional blindness rates of a subset of the conditions when using MTurk to those obtained when testing those exact conditions in a laboratory setting. Specifically, we took 6 conditions from our prior study that used the same experimental procedures (Cohen et al., 2021; (1) "Metamers" (small), 2) "Metamers" (large), 3) Texture-synthesis, 4) Inconsistent periphery, 5) Abstract periphery, and 6) Grey periphery) and compared the behavioral results with the data obtained in the present MTurk study. The correlation between the laboratory and MTurk inattentional blindness rates was remarkably high (r=0.98, P<0.0001; Supplemental Figure 3). The fact that the laboratory and MTurk data is almost perfectly correlated is critical, as it implies that our methods for examining inattentional blindness online are both valid and reliable.

Modeling behavior with deep convolutional neural networks (dCNNs).

How can we unify the behavioral results from these drastically different experimental conditions to form an overall understanding of perceptual awareness? To answer this question, we sought to build predictive models of these behavioral findings, which we could then probe to identify the specific visual features that determine the bandwidth of perceptual experience. We screened several dCNN architectures to predict the observed behavioral data. One major assumption of this approach is that these networks serve as a good approximation of the human visual system and learn a set of internal representations similar to those represented by the brain. This assumption is supported by numerous studies showing strong similarities between the human visual system and dCNNS (Khaligh-Razavi and Kriegeskorte, 2014; Güclü and van Gerven, 2015; Yamins and Dicarlo, 2016; Eickenberg et al., 2017; Greene & Hansen, 2018, Ratan Murty et al., 2021). Here, we followed the well-established encoding model framework to match the internal model features with the behavioral inattentional blindness rates. This modeling approach is comprised of two parts: 1) measuring the similarity between the features extracted for the original images and the altered images for each dCNN layer of a given network architecture and then 2) computing a linear mapping function between these similarity values and the behavioral measures (Figure 3). Each of these two parts are described below (see Methods).

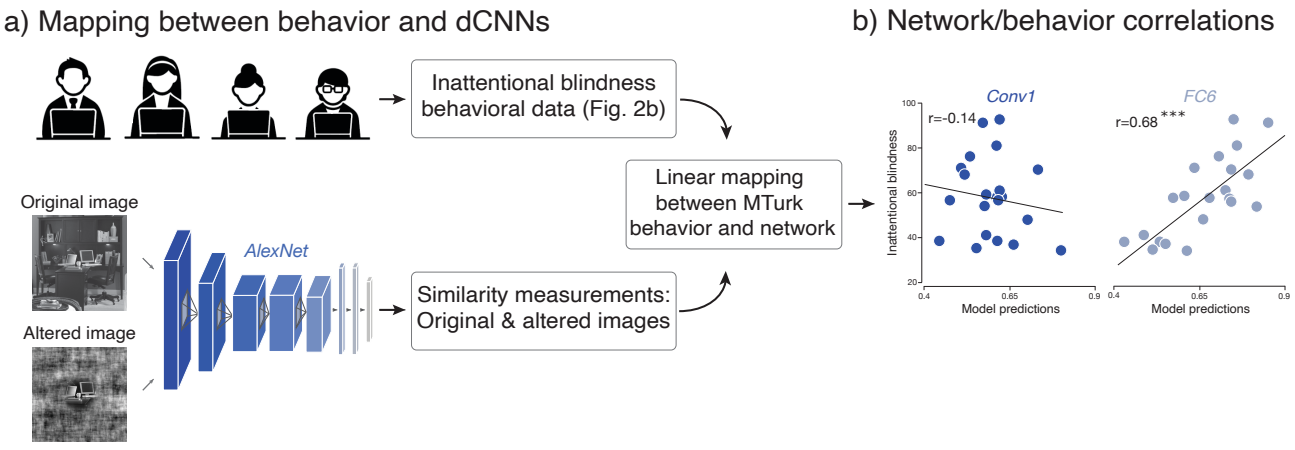

Figure 3. Outline of modeling procedures. a) To create a predictive model, we computed a direct linear mapping between the behavioral data obtained on MTurk (Fig. 2b) and the similarity measurements between

the original and altered images (see Methods). b) With this model, we then calculated the cross-validated predicted inattentional blindness rates and correlated them with the observed inattentional blindness rates.

To understand how we quantified the similarity between the original images and a given experimental condition (e.g., phase scrambled in the periphery), consider one layer of one network architecture (e.g., the first convolutional layer of AlexNet, see Methods). In this case, we first extracted the features for every individual original image and every altered image (Figure 3a). Then, for every individual original/altered image pairing (N=50 total pairs), we calculated the difference in the response magnitude across that layer. Next, we averaged across these difference values obtained for each of the 50 image pairings. The output of this averaging served as our similarity metric for a given experimental condition. Finally, these values were then turned into a vector and this process was then repeated for each of the 21 experimental conditions. Therefore, the final product of this procedure was a 21 x N matrix corresponding to the 21 experimental conditions and the number of features in a given layer of a particular network. To relate these similarity measurements to the behavioral data, we then used a Lasso regression to create a predictive model and tested each model's ability to predict held-out behavioral data (i.e., cross-validated, see Methods).

Which layers and features within a given network, if any, will best predict the behavioral data? To answer this question, we calculated the correlations between the observed inattentional blindness rates and the cross-validated predicted inattentional blindness rates made by a given layer in each network architecture (see Methods). This procedure was done with every layer of 7 different architectures: AlexNet, VGG-16, VGG-19, ResNet-18, SqueezeNet, DarkNet19, and MobileNet. These specific architectures were chosen because they are somewhat similar in their depth relative to other networks (e.g., ResNet-50, GoogleNet, InceptionV3, etc.), making it easier to directly compare these networks to one another. The results from this analysis are plotted in Figure 4. Across each network, we found that earlier layers could not successfully predict the behavioral data. However, the later layers were able to predict the behavioral data in each network we examined, with many of these layers reaching the behavioral noise ceiling. Since numerous studies have shown that dCNNs such as these gradually build up abstractions across layers (i.e., from simple edges to textures to patterns to object parts, etc., Yamins & DiCarlo, 2016), it strongly suggests that the key features that determine whether or not an observer notices alterations to the periphery are higher-level elements such as complex objects or even the spatial layout of a scene. In other words, these results suggest that the extent to which an observer will notice the alterations to the periphery is directly related to the extent to which higher-level elements of a scene are preserved. As those higher-level elements are themselves altered, it increases the likelihood that a particular alteration will be noticed. Meanwhile, lower-level features can be altered without observers noticing, so long as these higher-level elements are aspects of an image are preserved.

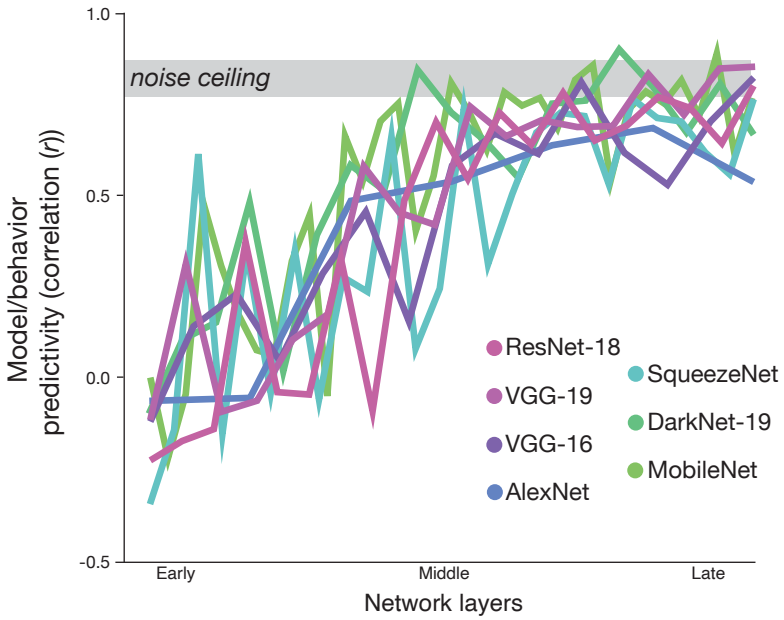

Figure 4. Model prediction accuracy for every network architecture. The vertical axis represents the correlation between the observed behavioral results and a model's prediction on held out data (i.e., cross-validated). The grey bar represents the behavioral noise ceiling (see Methods). The horizontal axis represents the specific layer of a given network architecture. Each colored line corresponds to a given network.

Feature visualization

A major advantage of using computational models like dCNNs is that we can directly probe them to investigate the specific features that are closely linked with perceptual awareness. Here, we identified the specific features that drive the model's ability to predict behavior and visualized those features to get an intuitive understanding of what they represent. Our results so far demonstrate that across a number of dCNN models, features in the late layers can be recombined to predict human behavioral performance (Figure 4). Given that we did not observe considerable differences across different architectures, we chose to only focus on VGG-19, one of the earliest and extensively studied dCNN model architecture, for subsequent analyses (Fig. 5a). Specifically, focused on the layer in this network that had the highest predictivity of the behavioral data relative to all other layers in the network (Conv5_3, see Fig. 4).

To identify the features with the most predictive power, we first examined the regression model weights between the model features and the behavioral data. Then, we selected the 10 features with the highest weights and found that restricting the analyses to just these 10 features could predict the behavioral data to the noise ceiling (correlation with behavior r=0.83, P<0.00001). While this finding demonstrates that only 10 features, which correspond to roughly 0.01% of the features in this layer, are sufficient to predict the human behavioral data, it leaves open the question of whether these features are truly necessary to predict the observed behavior. For instance, it is possible that there is enough redundancy within other features in this layer to also predict behavioral performance. We tested this necessity question in two ways. First, we used all but the XX features to re-learn a mapping between the model features and behavior. This analysis is akin to 'lesioning' specific neurons/sites.

We found a substantial drop in the ability to predict behavior from the 99.9% other features (r=0.60, P<0.01). Second, we randomly sub-sampled 10 features (without replacement) from available 99.9% model features, to balance the number of features for our tests. We observed an even steeper drop in the ability to predict the behavioral attentional blindness rates (correlation with behavior r=0.28, P=0.22). Together, these results provide strong evidence for a very small number of features (N = 10 features) in a late layer of VGG-19 being both necessary and sufficient to predict the behavioral inattentional blindness rates observed in our data.

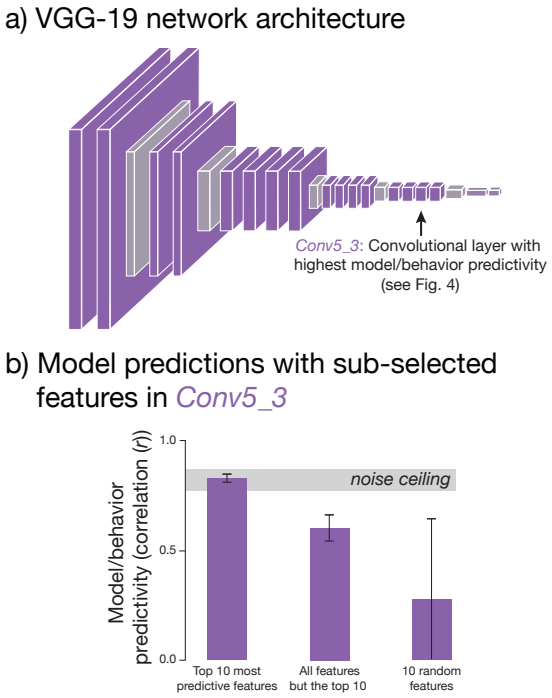

Figure 5. VGG-19 analysis: a) Sample architecture of VGG-19 with layer Conv5_3 indicated since it was the only analyzed layer in this analysis. b) The vertical axis represents the correlation between the observed behavioral results and a model's prediction on held out data (i.e., cross-validated). Each bar corresponds to a different set of features analyzed (i.e., the top 10 most predictive features, all features but the top 10, and 10 randomly selected features). The grey bar represents the behavioral noise ceiling (see Methods) and the error bars represent different iterations of the process.

This result still leaves open the question of what these 10 features represent. To answer this question, we used a version of feature visualization to determine what attributes of scenes the top 10 features are representing. Here, we chose to directly observe the strength of the gradients. The advantage of this method is that it provides maps that show the specific pixels that drive a given unit in a neural network the most. The pixel-level maps have higher resolution than other related methods like Grad-CAM, occlusion methods like LIME, and others. We reasoned that observing these high-resolution maps superimposed directly on the images used in our study would be particularly advantageous. Thus, we used a specific gradient attribution method called Guided Backpropagation (Springenberg et al., 2015; see Methods). The results from this analysis results in what we call 'Attribution maps' and can be visualized for a few example stimuli in Figure 6. Overall, the attribution maps, which highlight the particular parts of a scene that the top features are sensitive to, clearly focus on the outer contours of objects and scenes. For example, with an image of a canoe on a

lake, the attribution maps highlight the outer contours of the canoe itself but do not focus on the texture properties of the water, which has no strong outer contour. Conversely, with a picture of a beach, in which the horizon and shoreline serve as clear contours, the attribution maps highlight both of these aspects of the scene. Indeed, after examining several examples, it becomes clear that the critical elements are the contours of a scene (See Supplemental Figure 4 for attribution maps of every original image). In other words, the extent to which observers will notice alterations to an image appears to be linked to the extent to which those outer contours are preserved.

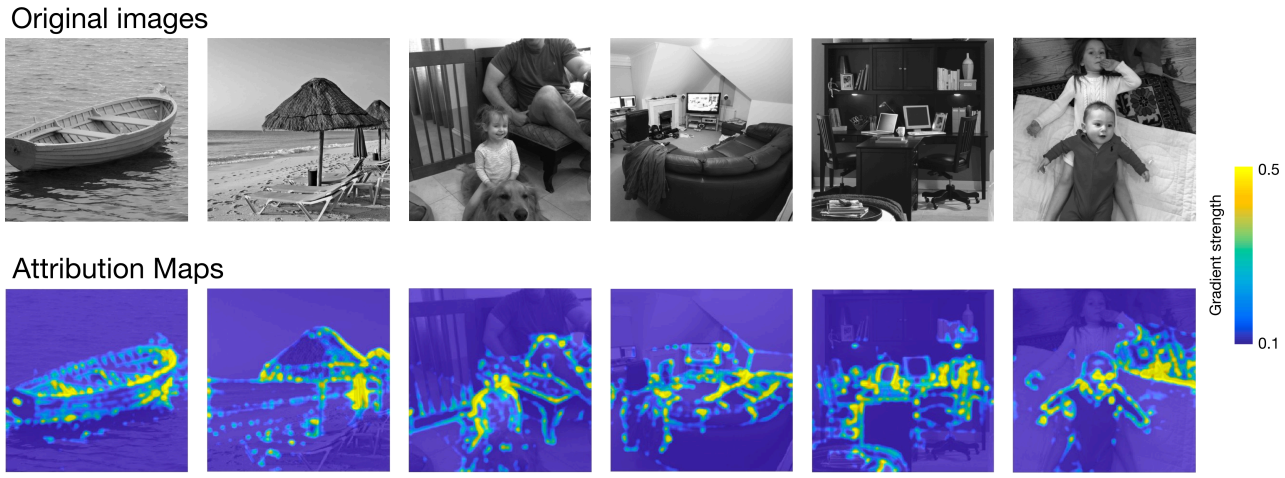

Figure 6. Feature visualization with attribution maps. On the top row are six example original images. On the bottom row are visualizations from the Guided Backpropogation procedures. The gradient strength is plotted from blue to yellow.

Discussion

Here, we examined the bandwidth of visual awareness using an inattentional blindness paradigm with natural scenes. Specifically, we altered the periphery of natural images in a wide variety of manners and measured how often observers noticed those alterations. To gain insight as to which aspects of natural scenes drive these results, we screened several dCNN architectures to create a series of predictive models. Within each of these architectures, we found that later layers and higher-level features, but not earlier layers or lower-level features, could predict the behavioral results extremely well, reaching the noise ceiling in many cases. In addition, we used feature visualization techniques to directly examine the features that had the most predictive power. Overall, this analysis revealed that these particular features represented the contours of higher-level elements of a scene, such as those of complex objects (e.g., chairs, couches, people, etc.) and the largest contours of a scene (e.g., the horizon, the shoreline, etc.). Taken together, these results suggest that the extent to which observers will notice alterations in the periphery is dictated by the extent to which higher-level features are preserved in a given condition and suggest that perceptual awareness is limited by higher level aspects of a scene.

Behavioral findings: One particular noteworthy aspect of the behavioral results is the extent to which observers often failed to notice drastic changes to the periphery. For example, observers a majority of observers failed to notice the periphery was scrambled so

much that no object in the periphery could be recognized (i.e., texture synthesis (Portilla & Simoncelli, 2001) or when the periphery was replaced with that of an entirely different scene. These results by themselves are important to emphasize since it has been previously claimed that even if an observer may fail to notice individual objects in a scene (i.e., change/inattentional blindness), they will still process the general "gist" of the scene (Mack & Rock, 1997; Simons & Levin, 1997; Koch & Tsuchiya, 2007; Sampanes et al., 2008; van Boxtel et al., 2010). Here, however, we find that this is often not the case and there are multiple instances when observers can fail to realize that a scene has been altered so thoroughly that it would drastically affect the meaning or interpretation of that scene. These findings suggest that a single snapshot of visual perception can be surprisingly impoverished. It should be stressed, however, that although this is not the first work to highlight the limits of perceptual awareness, no prior work has ever altered scenes in so many different ways in one set of experiments. Thus, these behavioral findings serve as an important benchmark for any theory of visual cognition that seeks to describe and characterize the overall bandwidth of visual awareness.

The benefits of modelling perceptual awareness: One of the difficulties in interpreting this set of behavioral data is because these numerous alterations occur along so many different perceptual dimensions (e.g., low-level vs higher-level changes). Such variation makes it difficult to understand how to synthesize these behavioral findings into a coherent whole. To deal with this difficulty, we used deep learning methods to create predictive models of inattentional blindness. Indeed, this is the first time that dCNNs have been use to study the limits of perceptual awareness with an inattentional blindness paradigm. Previous attempts to understand the bandwidth of perceptual awareness have often been underspecified in their attempts to describe the amount of information an observer is aware of at a given instant (Lamme, 2003; Koch & Tsuchiya, 2007; Block, 2011; Cohen et al., 2012; 2016; Haun et al., 2016). In other words, none of these prior frameworks could make explicit predictions about how often some alterations will be noticed relative to others (e.g., rotating the periphery 180° vs. passing the periphery through a low pass filter vs. phase scrambling the periphery, etc.). With so many different conditions altering the stimuli along a wide array of perceptual dimensions, it is difficult to know how these previous frameworks could successfully account for all of the behavioral data. With precise computational models, however, we have the capacity to shed light on the particular aspects of natural scenes play the largest role in determining whether or not observers will notice a set of alterations. In this case, the fact that later-layers predict inattentional blindness suggests that higher-level properties of a scene are the key features that enter perceptual awareness. So long as certain aspects of those features are preserved, alterations to the periphery will often go unnoticed.

Remaining questions and limitations: The results reported here raise several natural questions. One question asks, why are higher-level features more related to inattentional blindness performance than lower-level features? One possible reason is that a bottleneck based on higher-level aspects of a scene allows an observer to identify and function within a scene regardless of certain lower-level changes that may occur over time. For example, throughout any given day, the lighting may dramatically change from bright and sunny to overcast and hazy to dark and dim. However, across all these changes in the brightness, contrast, saturation, and intensity of the world, an observer can still often readily identify a

scene and act within it. Thus, the predictive power of later layers and higher-level features in the dCNNs can be interpreted as reflecting the fact that observers' perceptions of natural scenes are invariant to such lower-level changes.

This idea raises a second question: are we claiming that there are no instances in which perceptual awareness is limited by lower-level features? No. There are numerous methods related to visual awareness, such as backwards masking and crowding, that have been directly linked to early processing in the visual system (Breitmeyer & Ogen, 2006; Whitney & Levi, 2011). One integrative possibility is that there are multiple bottlenecks on perceptual awareness that can constrain conscious perception in several different ways. However, this fact does not take away from the main point we argue in this paper: specifically, the extent to which an observer will naturally notice alterations to a natural scene are determined by the extent to which higher-level properties of a given scene are preserved.

Finally, a natural question to wonder is, how might these results change if the primary task was different? Previously, Cohen et al (2020; 2021) had participants perform the same face/no-face task, as well as an indoor/outdoor task, in the same experimental setup as the one described here. When observers' attention was not focused around fixation (i.e., the face/no-face task) and was instead directed more towards the periphery (i.e., indoor/outdoor task), the rates of inattentional blindness dropped significantly. Since the primary task can drastically change the inattentional blindness rates, an intuitive question asks if different layers and features would best predict the behavior depending on the primary task. While we cannot answer this question definitively, and future research will be needed to determine this, we predict that the present pattern of results will hold regardless of the primary task. If this proves to be true, it would suggest that no matter the attentional state or task demands placed on an observer, perceptual awareness is limited by higher-level perceptual features. This prediction is somewhat supported by a recent study that used the attentional blink and also found that higher-level features best predict the magnitude of the attentional blink (Lindh et al., 2019). If instead, however, there were certain cases in which the exact same set of stimuli were used, but a different primary task made it such that earlier layers/features predicted behavior, it would suggest that the limits of perceptual awareness are flexibly dictated by the task an observer is performing at any given moment.

Conclusion: Together, this set of results helps elucidate the contents of perceptual awareness by building predictive models of inattentional blindness in natural scenes. Moreover, this study also demonstrates how using deep learning techniques can help understand the bandwidth of perceptual awareness. Going forward, it will be important for researchers to continue developing these tools in order to fully explain the contents of human visual consciousness.

Methods

Participants: 1,260 participants were recruited on Amazon's Mechanical Turk and were paid for their time. All participants were over 18 years old, gave informed consent, and indicated that they had normal or corrected-to-normal vision. All procedures of the experiment were performed in accordance with the Massachusetts Institute of Technology (MIT) Institutional Review Board and the Committee on the Use of Humans as Experimental Subjects.

Stimuli: *Critical stimuli for inattentional blindness:* Overall there were 21 experimental conditions with 50 stimuli per condition (see Figure 1 in main text and Supplemental Figure 1 for more examples):

1. "Metamers" (small): created using the Freeman and Simoncelli (2011) algorithm.
2. "Metamers" (medium): created using the Freeman and Simoncelli (2011) algorithm but changing the pooling region variable from 0.5 to 1.0.
3. "Metamers" (medium): created using the Freeman and Simoncelli (2011) algorithm but changing the pooling region variable from 0.5 to 3.0.
4. Texture synthesis: created using the Portilla and Simoncelli (2001) algorithm.
5. Gist texture: created using the Oliva and Torralba (2006) algorithm.
6. Phase scrambling: created using the Fourier transform to separate phase and amplitude information and preserving the amplitude while randomizing the phase.
7. Rotate the periphery 90°
8. Rotate the periphery 180°
9. Rotate the periphery 270°
10. White periphery (RGB values: 255, 255, 255)
11. Black periphery (RGB values: 0, 0, 0)
12. Grey periphery (RGB values: 127, 127, 127)
13. Diffeomorphic small: Morphing algorithm developed by Stojanoski & Cusak (2014) with a smaller 'maxdistortion' value.
14. Diffeomorphic big: Morphing algorithm developed by Stojanoski & Cusak (2014) a larger 'maxdistortion' value.
15. Inconsistent: the periphery of one image was placed around the middle part of the original images. These stimuli were initially created and used in our prior work (Cohen et al., 2021).
16. Inconsistent rotated 180°: the same inconsistent images, except the periphery was rotated 180°.
17. Abstract: the periphery was entirely replaced by two-tone abstract shapes and patterns. These stimuli were initially created and used in our prior work (Cohen et al., 2021).
18. Abstract desaturated: the same abstract images, except the opacity of the periphery was changed to 50% on top of a background of gray (RGB: 127, 127, 127).
19. Mooney periphery
20. Low pass filter periphery
21. High pass filter periphery

For each condition, an original set of 50 images always served as the starting point. 25 of those images had a face in the middle and 25 did not. All manipulations to these images occurred with the images subtending 26° of visual angle (although it was not necessarily the case that images were seen at this size in the experiment itself (see below)). To create all of the critical conditions, the center part of each original image was preserved by a flat top Gaussian that subtended 4° of visual angle (radius). The flat top portion of the Gaussian subtended 2.5° of visual angle (radius), which approximately corresponds to the fovea and was entirely unaltered. Meanwhile, the remaining 1.5° of visual angle were the slopes of the Gaussian served as a gradual fade from the untouched center of the image to the altered periphery of the image. This sloping/faded region comprised the remaining portion of the preserved region and would land approximately on the parafoveal part of the retina. All initial stimuli were acquired through online resources (i.e., Google) and personal photograph collections of the authors and were then converted to greyscale. See Supplementary Figures 1-2 for multiple examples of stimulus generation or procedures and example stimuli.

Face task stimuli: For the face detection task, the same stimulus set used in our prior work were used here (Cohen et al., 2021). There were 30 face target images and 30 distractor images. Each face target had

a human face that was unambiguously in the middle of the image, viewed either head on or from the side. Individual faces came from a variety of genders, ages, and ethnicities. Each no-face distractor was defined by not having a human face in the middle. In other words, there could be animal faces in the middle and humans in the periphery, but without a human face in the middle, those images were considered distractors. Before the experiment began, observers were shown multiple examples of both target and distractor images to understand what differentiated targets and distractors. For both face and no-face stimuli, the images comprised a wide variety of settings and locations (e.g., a man in a kayak, a construction worker, a chef in a kitchen, a dog on a dog bed, an empty office, an empty beach, etc.).

MTurk procedures: All observers were recruited and run online via Amazon Mechanical Turk. After initially agreeing to participants, all participants were redirected to a web server where platform-independent stimulus presentation and data collection were completed by custom software run in the web browser. All experiments were written using a combination of html and javascript. Since all stimuli were loaded on participants' own computers, viewing distance and screen resolution could dramatically different from one participant to the other. Thus, we simply chose to always make the images fit the full size of the screen.

Behavioral analyses: *Exclusion criterion:* For each of the 21 experimental conditions, data collection continued until we had recruited 60 participants who successfully completed the entire experiment (60 participants x 21 conditions = 1,260 total participants recruited). Every individual who participated in the experiment, regardless of whether or not they finished it, was precluded from ever participating in any other condition again. To be included in the final dataset, three criteria had to be met. First, an observer had to complete the entire experiment and answer all questions. Second, an observer had to complete the virtual chinrest, which was used to estimate an observer's viewing distance (Li et al., 2020). Finally, an observer had to get at least 8/10 of the face/no-face task correct on the 10 lead-up trials. This exclusion procedure was simply to have some sort of metric to ensure that participants were indeed paying attention to the screen and completing the task as instructed. Overall, this resulted in a total of 856 participants who met the exclusions criteria, which corresponds to 40.76 participants per condition. This number is similar to the one used in our prior work (Cohen et al., 2020; 2021), we obtained exactly 40 participants per condition in a laboratory setting. Moreover, these exclusion criteria were pre-registered before data acquisition began.

Noise ceiling: To determine the noise ceiling of the behavioral data, we calculated the split-half reliability amongst the participants who met the behavioral exclusion criterion. Within each of the 21 experimental conditions, we first divided the participants approximately in half and then computed the inattentional blindness rates for each half, resulting in a 2x21 matrix (2 splits of the data by 21 conditions). This procedure was repeated 1,000 times and the resulting average correlation of this procedure was then adjusted using the Spearman-Brown formula to estimate the split-half reliability of the full data set (Brown, 1910; Spearman, 1910). This adjusted value and its associated standard deviation served as the noise ceiling for all subsequent analyses (see grey bars in Figures 4 & 5 in the main text).

Modelling procedures: For each layer within each of the 7 dCNN architectures we tested, we build a model to try and predict the inattentional blindness behavior. To do this, we used a Lasso regression with a regularization hyperparameter set to 0.06. We then performed a 10-fold cross-validation (over 10 separate randomization seeds) to map the activations from each layer of every network to the behavioral data from the MTurk study. We used this particular method because of its relatively low computational cost and the fact that it seeks to capture the data using a simple, sparse model that relies on fewer features, which is well-suited for the lesioning analysis we performed (see below). In cases where we tested the pixel, Gist, Fourier, and HMAX models, we used the same Lasso regression procedures as those done with the dCNNs, but simply used the similarity between the original and altered images from these models into the regression.

References

Balas, B., Nakano, L., & Rosenholtz, R. (2009) A summary statistic-representaiton in peripheral vision explains visual crowding. *Journal of Vision*, 9, 13.

Block, N. (2011). Perceptual consciousness overflows cognitive access. *Trends in Cognitive Sciences,* 16, 567-575.

Breitmeyer, B., & Ogmen, H. (2006). Visual Masking: Time slices through conscious and unconscious vision. Oxford: Oxford University Press.

Castelhano, M.S., & Heaven, C. (2011). Scene context influences without scene gist: Eye movements guided by spatial associations in visual search. *Psychonomic Bulletin and Review,* 18, 890-896.

Chabris, C. F., Weinberger, A., Fontaine, M., & Simons, D. J. (2011). You Do Not Talk about Fight Club if You Do Not Notice Fight Club: Inattentional Blindness for a Simulated Real-World Assault. *I-Perception*, *2*(2), 150–153.

Cichy, R. M., Kriegeskorte, N., Jozwik, K. M., van den Bosch, J. J. F., & Charest, I. (2019). The spatiotemporal neural dynamicsunderlying perceived similarity for real-world objects. *Neuroimage*, 194, 12–24

Cohen, M.A. and Dennett, D.C. (2011) Consciousness cannot be separated from function. *Trends in Cognitive Sci*ences, 15, 358-364

Cohen, M.A., Cavanagh, P., Chun, M.M., & Nakayama, K. (2012). The attentional requirements of consciousness. *Trends in Cognitive Sciences,* 16, 411-417.

Cohen, M.A., Dennett, D.C, & Kaniwsher, N. (2016). What is the bandwidth of perceptual experience? *Trends in Cognitive Sciences,* 20, 324-335.

Cohen, M.A. & Rubenstein, J. (2020) How much color do we see in the blink of an eye? *Cognition*, 200, 104268.

Cohen, M.A., Ostrand, C., Frontero, N., & Pham, P-N. (2021) Characterizing a snapshot of perceptual experience. *Journal of Experimental Psychology: General*, 15, 1695-1709.

Dehaene, S., & Changeux, J.P. (2011). Experimental and theoretical approaches to conscious processing. *Neuron*. 70, 220-227.

Drew, T. & Stothart, C. (2016) Clarifying the role of target similarity, task relevance and feature-based suppression during sustained inattentional blindness. *Journal of Vision*, 16: 13.

Eickenberg, M., Gramford, A., Varoquaux, G., & Thirion, G. (2017) Seeing it all: Convolutional network layers map the function of the human visual system. *Neuroimage*, 152, 184-194.

Farzmahdi, A., Rajaei, K., Ghodrati, M., Ebrahimpour, R., & Khaligh-Razavi, S-M. (2016) A specialized face-processing model inspired by the organization of monkey face patches explains several face-specific phenomena observed in humans. *Scientific Reports,* 6, 25025.

Fischer, Edith, Richard F. Haines, and Toni A. Price. (1980) Cognitive Issues in Head-Up Displays. *Nasa Technical Paper*, 1711, 1-28.

Freeman, J., & Simoncelli, E.P. (2011). Metamers of the ventral stream. *Nature Neuroscience,* 14, 1195-1201.

Güclü, U., & van Gerven, A.J. (2015) Deep neural networks reveal a gradient in the complexity of neural representations across the ventral stream. *Journal of Neuroscience*, 35, 10005-10014.

Greene, M. & Hansen, B.C. (2018) Shared spatiotemporal category representations in biological and artificial deep neural networks. *PLoS Computational Biology*, 14, 7.

Haun, A.M., Tononi, G., Koch, C., Tsuchiya, N. (2017). Are we underestimating the richness of visual experience? *Neuroscience of Consciousness,* doi: 10.1093/nc/niw023.

Hayhoe, M.M., Shrivastava, A., Mruczek, R., & Pelz, J. (2003). Visual memory and motor planning in a natural task. *Journal of Vision.* 3, 49-63.

Henderson, J.M. (2003). Human gaze control during real-world scene perception. *Trends in Cognitive Sciences,* 7, 498-504.

Itti L, Koch C. Computational modeling of visual attention. *Nat Rev Neurosci* 2: 194-203, 2001.

Jacob, G., Pramod, R.T., Katti, H., & Arun, S.P. (2021) Qualitative similarities and differences in visual object representations between brains and deep networks. *Nature Communications*, 12, 1-14.

Jensen, M.S., Yao, R., Street, W.N., & Simons, D.J. (2011). Change blindness and inattentional blindness. *WIREs Cognitive Science,* 2, 529-546.

Jozwik, K., Kriegeskorta, N., Storrs, K., & Mur, M. (2017) Deep convolutional neural networks outperform feature-based but not categorical models in explaining object similarity judgments. *Frontiers in Psychology*, 8, 1726.

Khaligh-Razavi, S-M & Kriegeskorte, N. (2014) Deep supervised, but not unsupervised, models may explain IT cortical representation. *PLoS Computational Biology*, 6, 10.

Koch, C., & Tsuchiya, N. (2007). Attention and consciousness: two distinct brain processes. *Trends in Cognitive Sciences,* 11, 16-22.

Knotts, J.D., Odegaard, B., Lau, H., & Rosenthal, D. (2019). Subjective inflation: phenomenology's get-rich-quick scheme. *Current Opinion in Psychology,* 29, 49-55.

Kubilius, J., Bracci, S., & Op de Beeck, H.P. (2016) Deep neural networks as a computational model for human shape sensitivity. *PLoS Computational Biology*, 12:e1004896.

Lamme, V. A. F. (2003) Why visual attention and awareness are different. *Trends in Cognitive Sciences,* 7, 12-18.

Levin, D. T., Momen, N., Drivdahl, S. B., & Simons, D. J. (2000). Change Blindness Blindness: The Metacognitive Error of Overestimating Change-detection Ability. *Visual Cognition*, *7*(1–3), 397–412. https://doi.org/10.1080/135062800394865

Lindh, D., Sligte, I., Assecondi, S., Shapiro, K. & Charest, I. (2019) Conscious perception of natural images is constrained by category-related visual features. *Nature Communications*, 10, 4106.

Luck, S.J. and Vogel, E.K. (2013) Visual working memory capacity: from psychophysics and neurobiology to individual differences. *Trends Cogn. Sci.* 17, 391-400

Mack, A. & Rock, I. (1998). *Inattentional Blindness*. MIT Press: Cambridge.

Most, S.B., Scholl, B.J., Clifford, E.R., & Simons, D.J. (2005) What you see is what you set: Sustained inattentional blindness and the capture of awareness. *Psychological Review*, 112, 217-242.

Nuthmann, A. (2017). Fixation durations in scene viewing: Modeling the effects of local image features, oculomotor parameters, and task. *Psychonomic Bulletin and Review,* 24, 370-392.

O'Regan, J.K., Rensink, R.A., & Clark, J.J. (1999) Change blindness as a result of 'mudsplashes.' *Nature*, 398, 34.

Oliva, A, & Torralba, A. (2001) Modeling the shape of the scene: A holistic representation of the spatial envelope. *International Journal of Computer Vision*, 42, 145-175.

Oliva, A, & Torralba, A. (2006) Building the gist of a scene: The role of global image features in recognition. *Progress in Brain Research*, 155, 23-36.

Pelz, J.G., & Canosa, R. (2001). Oculomotor behavior and perceptual strategies in complex tasks. *Vision Research,* 41, 3587-3596.

Rajalingham, R., Issa, E.B., Bashivan, P., Kar, K., Schmidt, K., & DiCarlo, J. (2018) Large-scale, high-resolution comparison of the core visual object recognition behavior of humans,

monkeys, and state-of-the-art deep artificial neural networks. *Journal of Neuroscience*, 38, 7255-7269.

Ratan Murty, N.A., Bashivan, P., Abate, A., DiCarlo, J. & Kanwisher, N. (2021) Computational models of category-selective brain regions enable high-throughput tests of selectivity. *Nature Communications*, 12, 1-14.

Rayner, K. (1998). Eye movements in reading and information processing: 20 years of research. *Psychological Bulletin,* 124, 372-422.

Rayner, K., Smith, T.J., Malcolm, G.L., & Henderson, J.M. (2008). Eye movements and visual encoding during scene perception. *Psychological Science,* 20, 6-10.

Rensink, R., O'Regan, J.K., & Clark, J.J. (1997). To see or not to see: The need for attention to perceive changes in scenes. *Psychological Science,* 8, 368-373.

Rosenholtz, R. (2020) Demystifying visual awareness: Peripheral encoding plus limited decision complexity resolve the paradox of rich visual experience and curious perceptual failures. *Attention Perception, and Psychophysics,* 82, 901-925

Sampanes, A.C., Tseng, P., & Bridgeman, B. (2008) The role of gist in scene recognition. *Vision Research*, 48, 2275-2283.

Simons, D., & Levin, D. (1997). Change blindness. *Trends in Cognitive Sciences*, 1, 261–267.

Simons, D.J. and Chabris, C.F. (1999) Gorillas in our midst: sustained inattentional blindness for dynamic events. *Perception* 28, 1059-1074

Simons, D. J., Franconeri, S. L., & Reimer, R. L. (2000). Change Blindness in the Absence of a Visual Disruption. *Perception*, *29*(10), 1143–1154.

Simons, D.J., & Rensink, R. (2005). Change blindness: Past, present, and future. *Trends in Cognitive Sci*ences, 9, 16-20.

Springenberg, J.T., Dosovitskiy, A., Brox, T., & Riedmiller, M. (2015) Striving for Simplicity: The All Convolutional Net. ArXiv: http://arxiv.org/abs/1412.6806.

Unema, P.J.A., Pannasch, S., Joos, M., & Velichkovsky, B.M. (2005). Time course of information processing during scene perception: The relationship between saccade amplitude and fixation duration. *Visual Cognition,* 12, 473-494.

Van Boxtel, J.A., Tsuchiya, N., & Koch, C. (2010) Consciousness and attention: on sufficiency and necessity. *Frontiers in Psychology*, 1,1-13

Ward EJ, Scholl BJ (2015) Inattentional blindness reflects limitations on perception, not memory: Evidence from repeated failures of awareness. *Psychon Bull Rev* 22,722–727.

Whitney, D. & Levi, D. M. (2011) Visual crowding: a fundamental limit on conscious perception and object recognition. *Trends Cogn. Sci.* 15, 160–8

Wolfe JM (1999) Inattentional amnesia. *Fleeting Memories: Cognition of Brief Visual Stimuli.*, MIT Press/Bradford Books series in cognitive psychology. (The MIT Press), pp 71–94.

Yamins, D.L.K. & DiCarlo, J.J. (2016) Using goal-driven deep learning models to understand sensory cortex. *Nature Neuroscience*, 19, 356-365.

Zhang, X., Huang, J., Yigit-Elliott, S., & Rosenholtz, R. (2015) Cube search, revisited. *Journal of Vision*, 15, 9.

Supplemental material

Modeling the bandwidth of perceptual experience using deep convolutional neural networks

Michael A. Cohen[1,2], Kirsten O. Lydic[1], & N. Apurva Ratan Murty[1]

[1] McGovern Institute for Brain Research, Department of Brain and Cognitive Sciences, Massachusetts Institute of Technology

[2] Department of Psychology and Program in Neuroscience, Amherst College

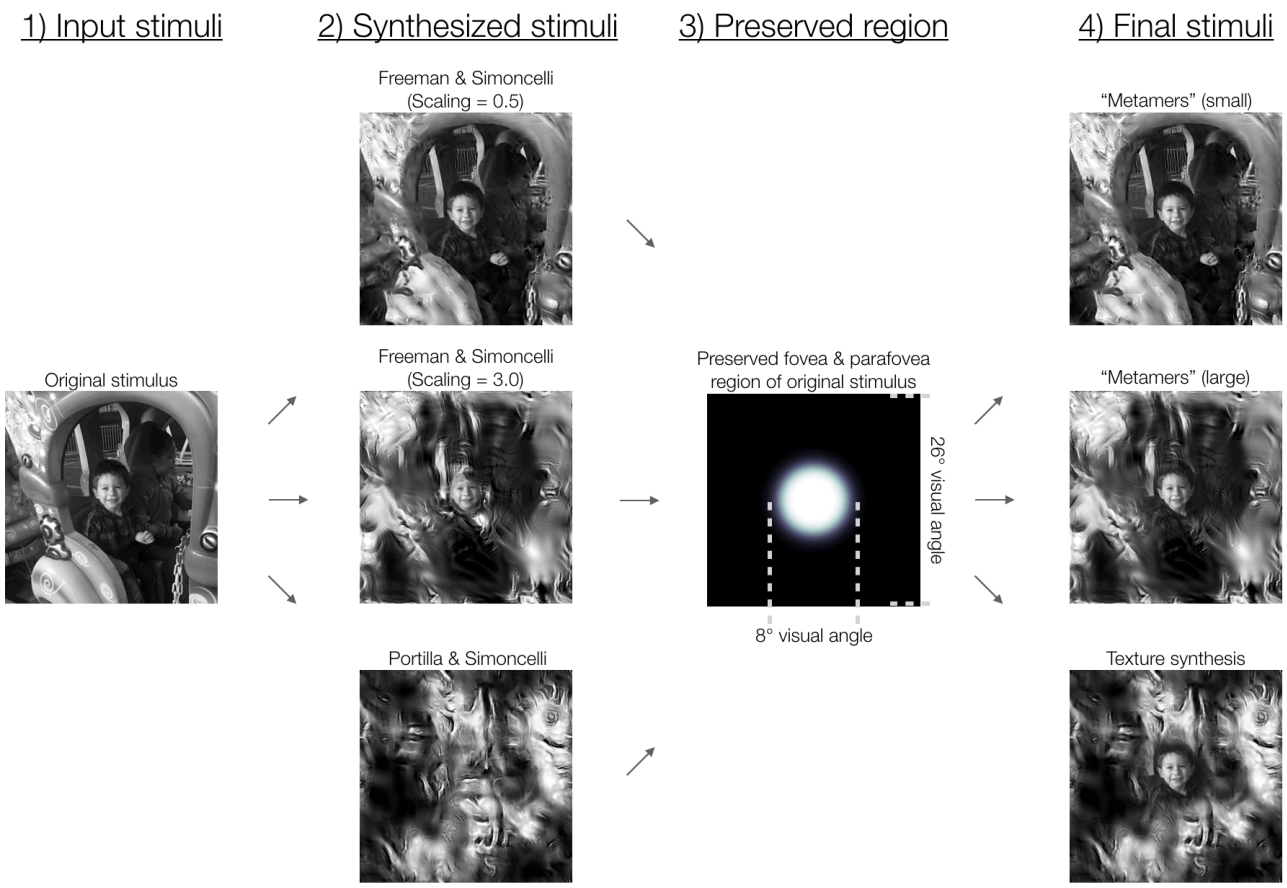

Supplemental Figure 1. Stimulus generation procedures using texture synthesis algorithms. 1) An original stimulus was chosen and cropped to be the appropriate size. 2) That stimulus was then run through our different texture synthesis algorithms: a) *"Metamers" (small)*, which used the Freeman and Simoncelli algorithm with a scaling parameter of 0.5, b) *"Metamers" (large)*, which also used the Freeman and Simoncelli algorithm but with a scaling parameter of 3.0, and c) *Texture synthesis*, which used the Portilla and Simoncelli algorithm. 3) Furthermore, a preserved part of the original stimulus was then selected that corresponded to the size of the fovea/parafovea that subtended 8 degrees of visual angle. 4) The preserved portion of the original stimulus and scrambled stimuli from the texture synthesis algorithms were then combined to create the final stimuli used in the experiments.

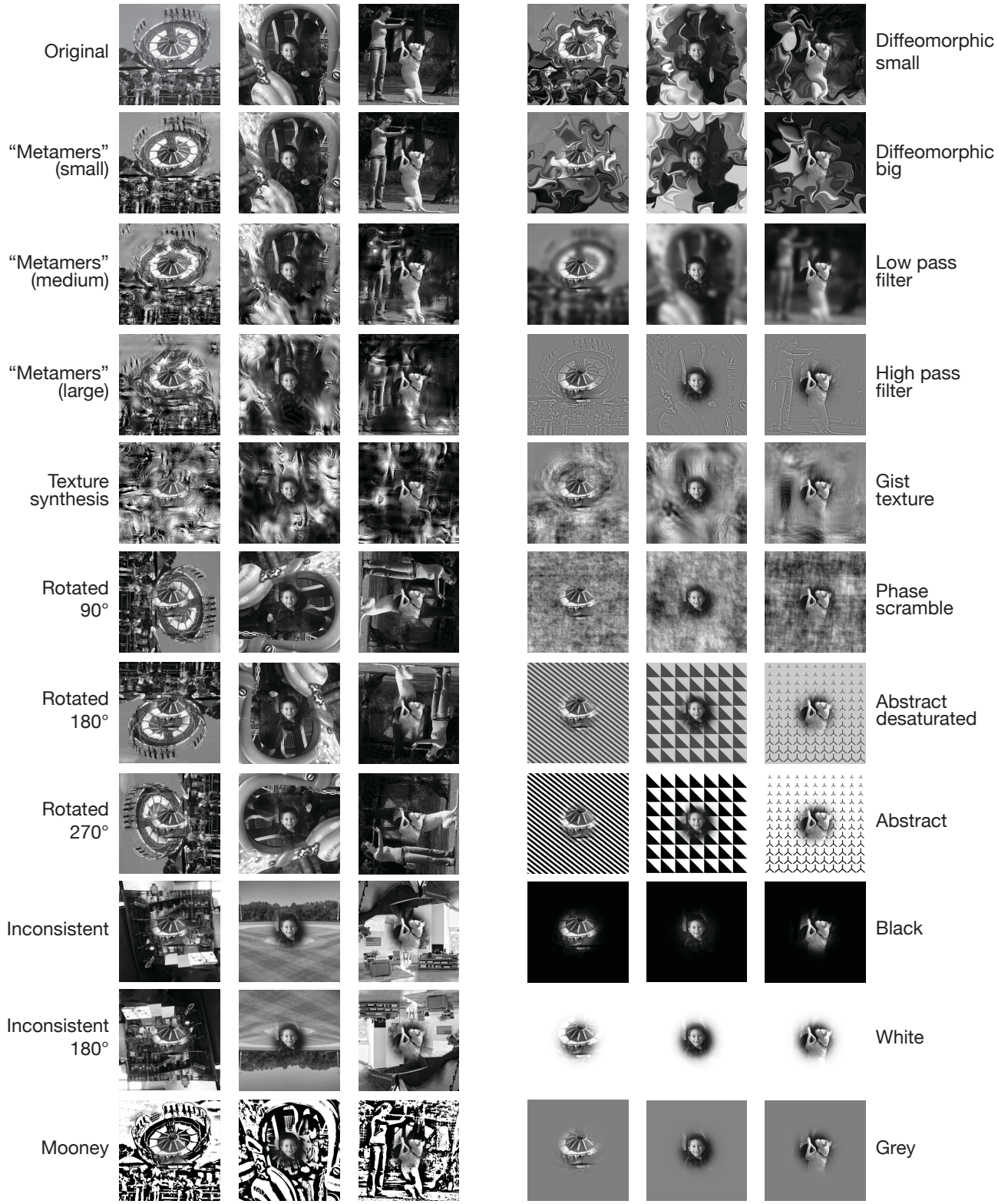

Supplemental Figure 2. Examples from each experimental condition. Original images are shown on the top left, with an example of that image then being altered in each of the 21 different experimental condition.

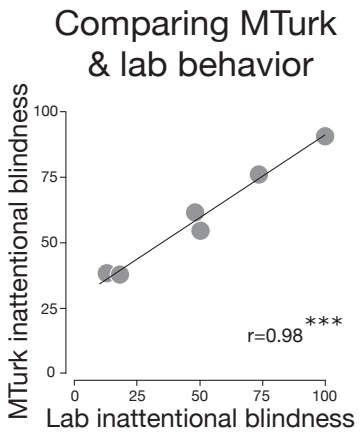

Supplemental Figure 3. Correlation between inattentional blindness rates with six conditions when tested in the laboratory (x-axis) and MTurk (y-axis).

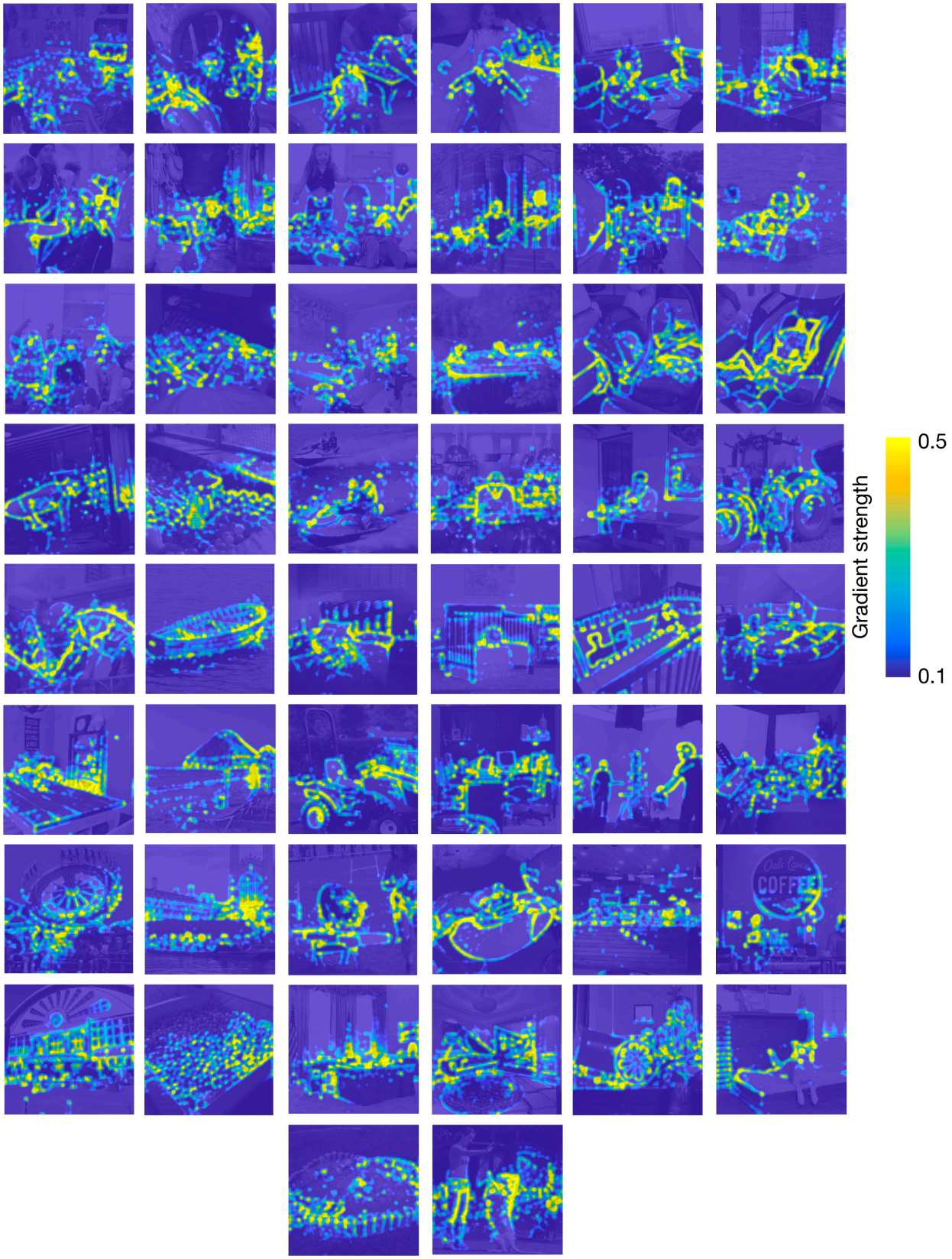

Supplemental Figure 4. visualizations from the Guided Backpropogation procedures for every original image used in the experiment. The gradient strength is plotted from blue to yellow.